

Quasicrystals and crystalline phases in $\text{Al}_{65}\text{Cu}_{20}\text{Fe}_{10}\text{Cr}_5$ alloy

C. DONG*[†], J. M. DUBOIS[†]

**Institut Laue-Langevin, 156X, 38042 Grenoble, France*

[†]*Laboratoire de Metallurgie, Ecole des Mines, Parc de Saurupt, 54042 Nancy, France*

An alloy of composition $\text{Al}_{65}\text{Cu}_{20}\text{Fe}_{10}\text{Cr}_5$ forms a mixture of icosahedral and decagonal quasicrystals upon rapid solidification from the liquid state. These quasicrystals are highly faulted as revealed by electron microscopy studies. After heat treatment, the alloy transforms into a new orthorhombic modification. This crystal is studied by X-ray and transmission electron microscopy and emphasis is put on its close resemblance to the decagonal phase.

1. Introduction

It has been reported that a new stable icosahedral phase is formed in Al-Cu-Fe alloys even by conventional solidification [1]. Since the historical discovery of the icosahedral phase in a rapidly solidified Al-Mn alloy by Shechtman *et al.* [2], several kinds of quasicrystals have been found in many alloy systems [3]. Besides the icosahedral phase which is the three-dimensional quasicrystal with $m\bar{3}5$ point group symmetry, two-dimensional quasicrystals (decagonal phase [4], dodecagonal phase [5] and octagonal phase [6]) and one-dimensional quasicrystal [7] have also been reported. Most of these quasicrystals can, however, be obtained only by out of equilibrium preparation methods such as spin-quenching, ion implantation and sputtering [7]. Very few of them, namely the icosahedral phase in Al-Li-Cu [8] and Ga-Mg-Zn [9] alloy systems, are stable. The icosahedral phase in Al-Cu-Fe system is of particular interest because it appears to have a very perfect quasicrystalline structure [10]. The present investigation concentrates on the addition of chromium in substitution to iron (5 at. %) on the structure of the rapidly solidified and subsequently heat-treated samples by means of transmission electron microscopy (TEM) and X-ray diffraction.

2. Sample preparation

An alloy with nominal composition $\text{Al}_{65}\text{Cu}_{20}\text{Fe}_{10}\text{Cr}_5$ was prepared in an evacuated RF furnace. Rapid solidification was realized by the melt-spinning technique. The samples for TEM observation were prepared by the standard thinning method. The electron microscope used is a J200cx installed with high resolution polar pieces so that both high resolution electron microscopy (HREM) and large angle double-tilting experiments could be carried out simultaneously. The X-ray measurements were done by using a cobalt target with wave length of 0.178 894 nm. In order to test the thermal stability of the samples, the melt-spun samples were annealed at 1200 K for 3 h

and then slowly cooled to room temperature at a cooling rate of 0.2 K min^{-1} , so that one can expect the resultant samples to be in an equilibrium state.

3. Results and discussion

3.1. As-quenched samples

The as-quenched samples consist mainly of icosahedral phase (i-phase) and decagonal phase (d-phase), as detected both by X-ray diffraction and TEM examination. The amount of d-phase is larger than that of i-phase.

3.1.1. *i*-phase

Its morphology is characterized by grains up to $1 \mu\text{m}$ in size with irregular shape as marked by "i" in Fig. 1. Systematic tilting along different axes results in a series of electron diffraction patterns (EDPs) which confirm the icosahedral point group symmetry. Typical EDPs thus obtained are shown in Fig. 2. These patterns reveal that the i-phase is rather imperfect. Severe deviation from τ ratio on the EDPs is obvious. For instance, the 3f EDP is almost periodic and the 5f EDP has a lot of discrete spots. The latter phenomenon is frequently observable during decomposition of the i-phase upon heating, thus the i-phase is in a transition state towards crystallization. Fig. 3 shows three 2f EDPs which have periodicity modulated along one or two 5f axes. Fig. 3c is in fact a periodic pattern with periodicity along both of the 5f axes so that this pattern is from domains of a true crystalline phase, though the diffraction intensities still remain in a Fibonacci sequence. Coincidentally, the 3f EDP in Fig. 2 is also periodic and it seems that there exist domains of an unknown crystalline phase. The HREM image taken along the 2f direction of the i-phase confirms the above diffraction analysis. As shown in Fig. 4, the i-phase is highly faulted and has local periodic ordering (with scale up to more than ten nanometres) in one or two directions; the angle between them agrees with that between two 5f directions

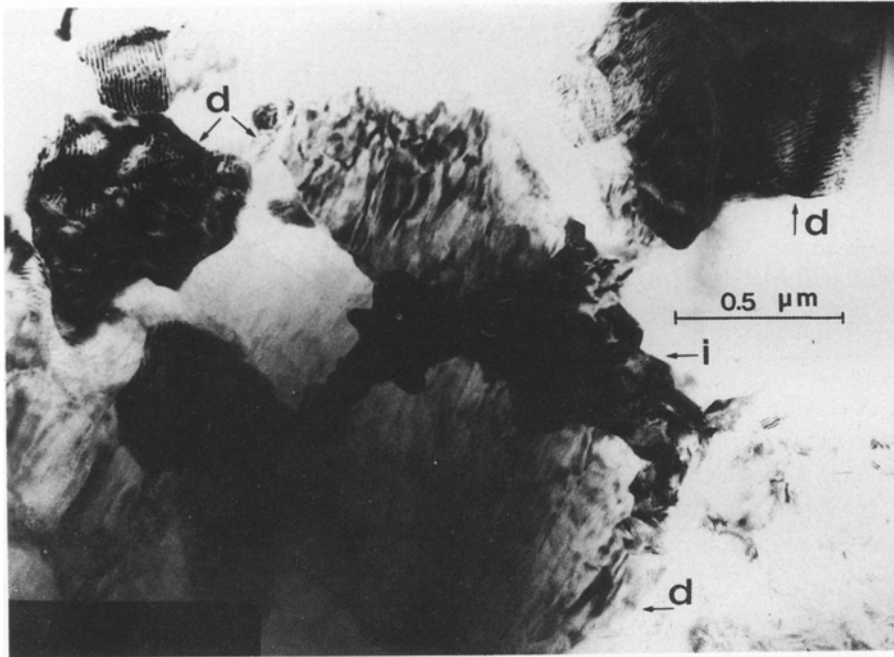


Figure 1 The bright-field image of Al₆₅Cu₂₀Fe₁₀Cr₅ melt-spun sample. Icosahedral phase and decagonal phase are marked by "i" and "d" respectively.

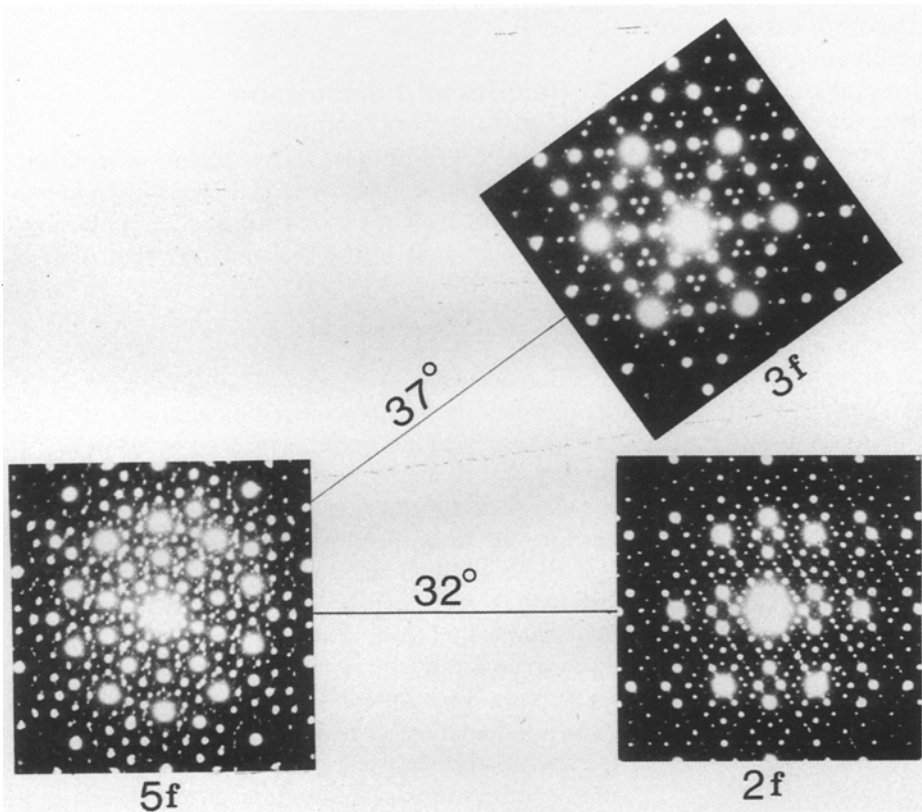


Figure 2 Typical electron diffraction patterns of imperfect icosahedral phase. Severe distortion from ideal τ ratio can be observed.

(63.4°). The periodicity along one or two 5f axes on the 2f patterns in Fig. 3 is therefore due to the presence of regions of different states of ordering, with the ultimate state of full crystallization which corresponds to an unknown crystalline phase. Zhang and Kuo [11] have observed local transitional ordering during the transformation of the i-(Ni, Ti, V) phase to crystalline phases. The periodicity, however, occurs along the 2f direction rather than the 5f direction as in our case. This may reflect the fact that these two i-phases are different in structure, with the latter having a unique bcc reciprocal lattice [12].

3.1.2. d-phase

The d-phase has a stripy appearance typical of d-phases as marked by "d" in Fig. 1. The d-phase grains are usually about 1 μm in diameter, often in massive shape and can be identified easily from that characteristic morphology. In many cases, they coexist and have an orientation relationship with the i-phase, which has been well studied by Schaefer and Bendersky [13] and Guyot and Audier [14]. Although the X-ray diffractogram can be indexed accurately with d-phase notation, the EDPs show that local periodic ordering also occurs. Fig. 5a and 5b

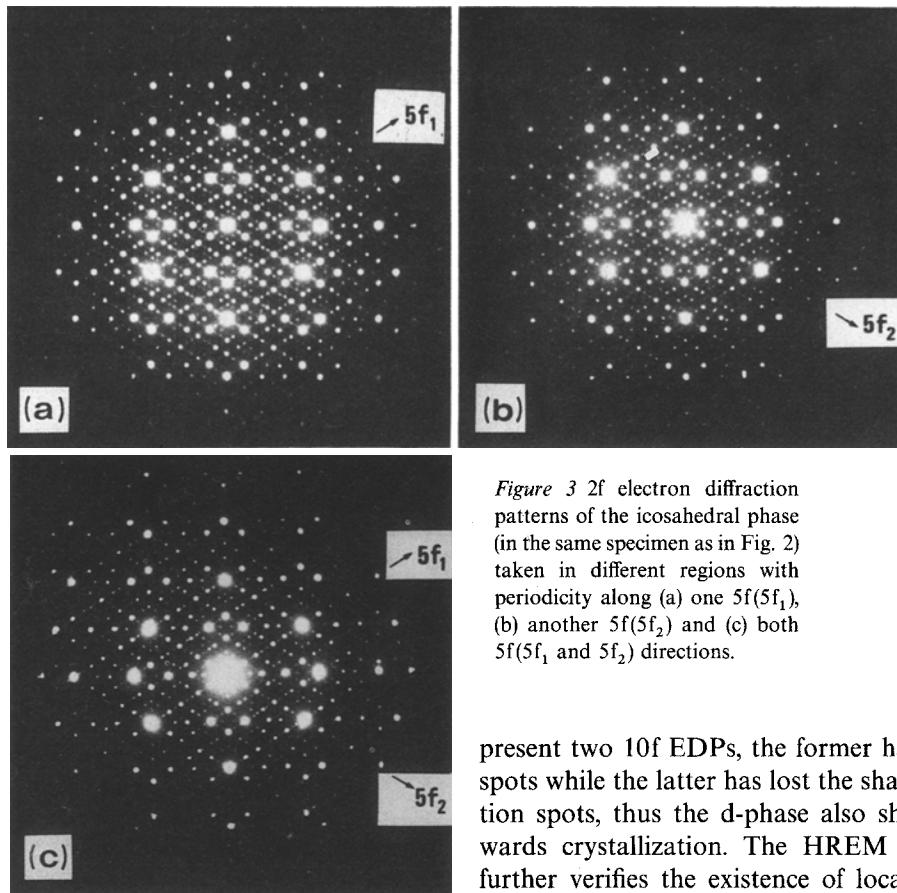


Figure 3 2f electron diffraction patterns of the icosahedral phase (in the same specimen as in Fig. 2) taken in different regions with periodicity along (a) one $5f(5f_1)$, (b) another $5f(5f_2)$ and (c) both $5f(5f_1)$ and $5f_2$ directions.

present two 10f EDPs, the former has many discrete spots while the latter has lost the sharpness of diffraction spots, thus the d-phase also shows a trend towards crystallization. The HREM image of Fig. 4 further verifies the existence of local crystalline domains in d-phase grains as well as a coexisting crystalline phase grain which is denoted as O-phase. Though the O-phase is rare in the as-quenched samples, its occurrence is not accidental: Thangaraj *et al.* [15] have noticed this phase in Al-Mn melt-spun ribbons, but they did not examine it in any detail and a similar phase was also found in sputtered Al-Mn thin films [16, 17]. The close relation between d-phase and O-phase in existing morphology, diffraction pattern and HREM image seem to support the suggestion that O-phase may be the close approximate crystalline phase of d-phase and such a point is proved by subsequent heat treatment with the result that these samples massively contain the O-phase and both i-phase and d-phase have disappeared.

Compared to the $Al_{65}Cu_{20}Fe_{15}$ alloy which forms a perfect, stable i-phase with dodecahedral morphology, the addition of chromium in substitution to iron destabilizes the i-phase and promotes the formation of the d-phase. In our samples, we found that both phases are in transition states towards periodic ordering and one can expect their decomposition upon sufficient heat treatment.

3.2. Heat treated samples

The as-quenched samples were annealed at 1200 K for 3 h then slowly cooled to room temperature at a rate of 0.2 K min^{-1} . The resultant samples consist of, as determined by X-ray diffraction, "pure d-phase". The X-ray diffractogram shown in Fig. 6 can well be indexed with d-phase notation [18]. As listed in Table I, the indexing agrees perfectly with the d-phase, with an error normally less than 0.001 nm in lattice spacing values. Notice also the close resemblance between this

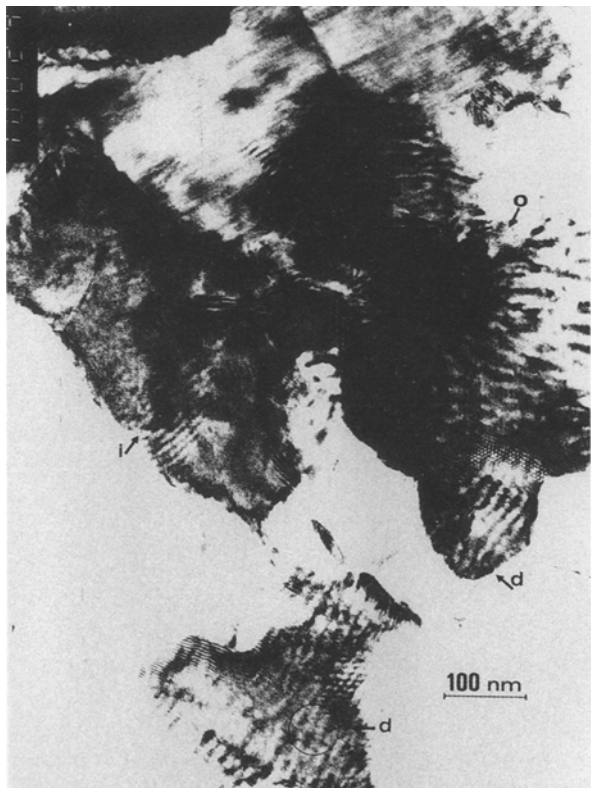


Figure 4 The high resolution image of a group of coexisting icosahedral, decagonal and O-phase grains taken along their common 2f axis. Some typical local periodic ordering regions are circled. Two 5f directions are marked by $5f_1$ and $5f_2$ which coincide with diffraction analysis (see Fig. 3).

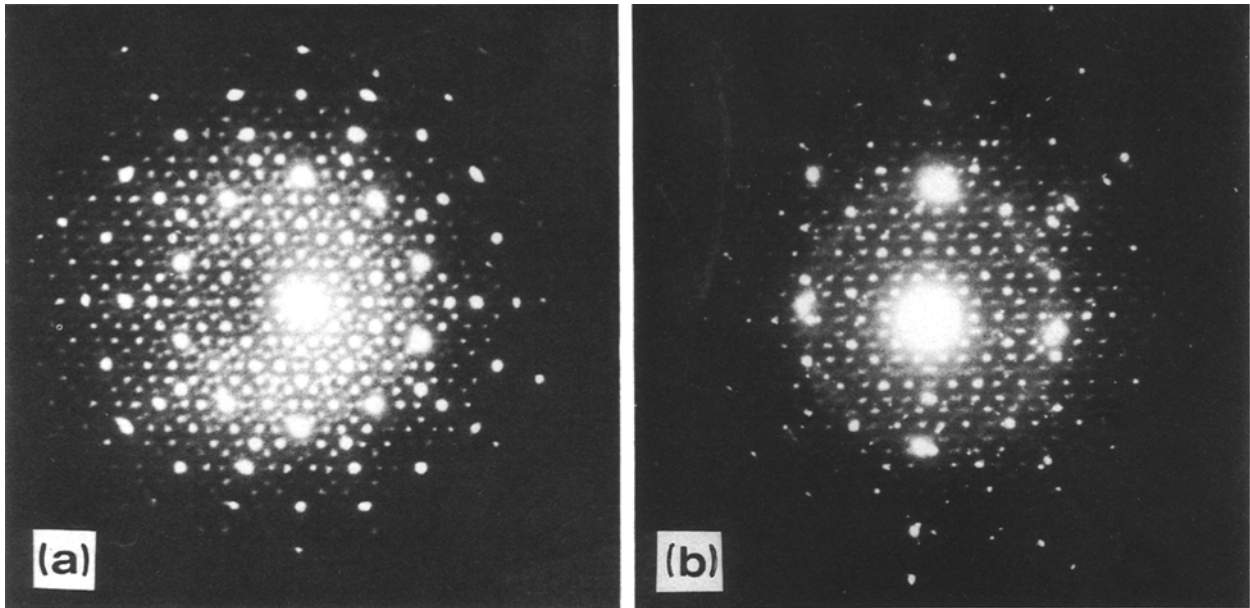


Figure 5 Two 10f diffraction patterns of decagonal phase in the as-quenched sample. Both of them show severe deviations from ideal decagonal phase. The latter is obviously more decomposed.

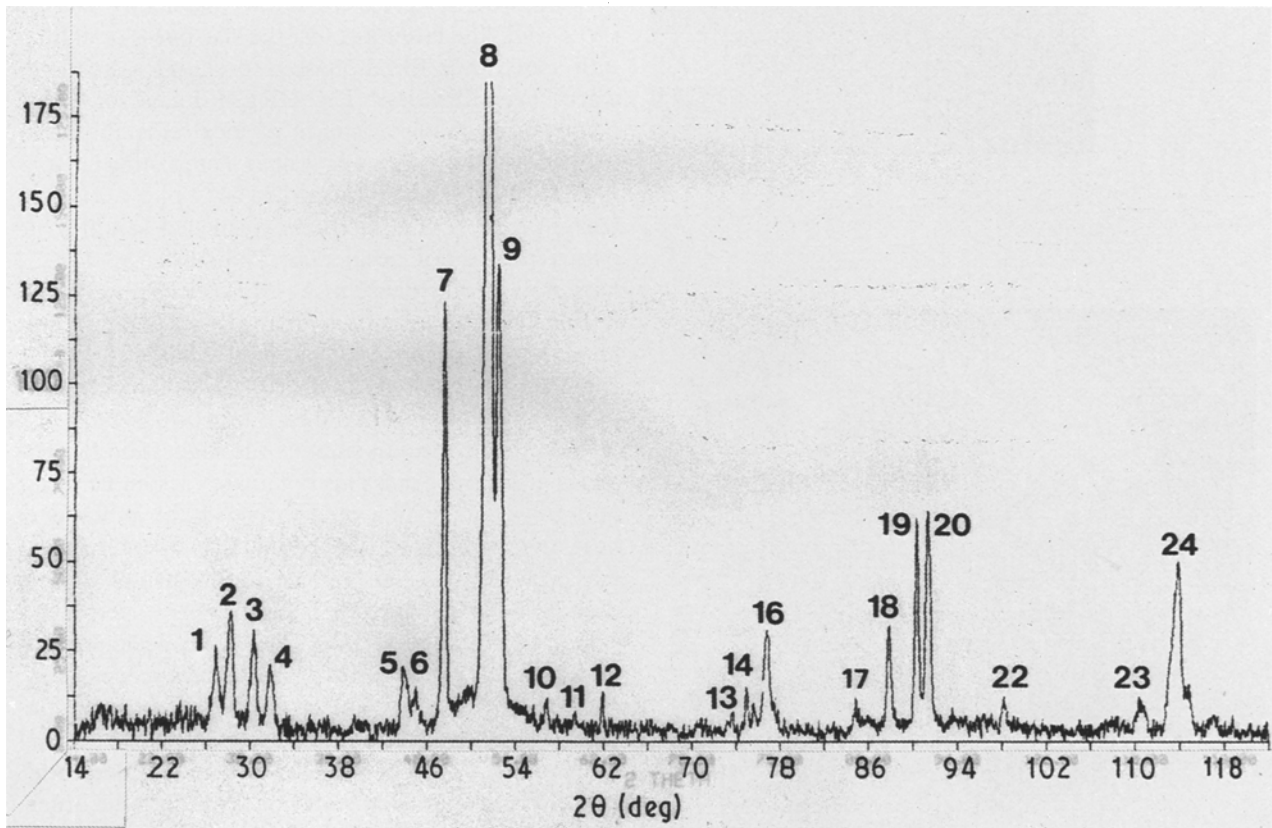


Figure 6 X-ray powder diffraction diagram of the heat treated sample. The indexation is listed in Table I.

diffraction pattern and the one measured with metastable $Al_{80}Mn_{20}$ decagonal phase [19]. TEM analysis, however, identifies another crystalline phase, named O-phase, which already exists in as-quenched samples as a minority phase (Fig. 4). Thus this crystalline phase is so good an approximation to the d-phase that the difference is beyond what the normal X-ray diffraction experiment can tell! The EDPs also much resemble those of the d-phase both in positions of intense reflections and angles between the typical zone

axes. By large angle double tilting of the sample in the microscope, a series of EDPs have been obtained as shown in Fig. 7. The three-dimensional reciprocal space can accordingly be reconstructed which leads us to the conclusion of a B base-centred orthorhombic phase with lattice parameters $a = 2.365$ nm, $b = 1.228$ nm, $c = 3.250$ nm (these values have been further refined by using X-ray data). Similar phases found previously have the same orthorhombic structure but without a B base-centre, with the result that the a and b lattice

TABLE I Indexations of X-ray diffractogram using both O-phase and d-phase notation

No	Experimental			O-phase ^a		d-phase ^b	
	2 θ (deg)	<i>D</i> (nm)	Int ^c	Index	<i>D</i> _{cal} (nm)	Index	<i>D</i> _{cal} (nm)
1	26.88	0.3849	6.0	505	0.3825	12210	0.3849
2	28.22	0.3669	8.3	515	0.3652	12211	0.3673
3	30.31	0.3421	7.0	333	0.3444	01103	0.3421
4	31.80	0.3265	5.3	525	0.3265	02210	0.3274
5	43.92	0.2392	4.5	808	0.2390	12212	0.3262
						12214	0.2401
6	45.01	0.2337		818	0.2346	13310	0.2379
						13311	0.2335
7	47.56	0.2218	28.1	828	0.2227	13312	0.2218
8	51.56	0.2057	100	838	0.2064	13313	0.2045
				060	0.2046	00006	0.2057
9	52.45	0.2024	30.5	00.16	0.2031	13420	0.2024
10	56.67	0.1885		848	0.1886	13314	0.1881
11	59.29	0.1808		565	0.1804	12216	0.1807
12	61.94	0.1738	3.1	103.10	0.1732	02423	0.1745
13	73.38	0.1497		383	0.1492	00118	0.1489
14	74.99	0.1470	3.4	130.13	0.1471	25520	0.1470
15	75.41	0.1462		13.1.13	0.1461	25521	0.1460
16	76.83	0.1440	7.0	06.16	0.1442	14523	0.1443
						13426	0.1439
17	84.53	0.1330		134.13	0.1327	25524	0.1326
18	87.83	0.1290	7.3	888	0.1291	13318	0.1290
						12219	0.1286
19	90.33	0.1261	14.2	135.13	0.1262	25525	0.1262
20	91.36	0.1250	14.7	00.26	0.1250	15630	0.1251
21	93.28	0.1230		010.0	0.1228	0000.10	0.1227
22	98.06	0.1185		898	0.1185	26621	0.1184
						13319	0.1184
23	110.16	0.1091		8.10.8	0.1227	133110	0.1091
						26732	0.1090
						14528	0.1088
24	113.89	0.1067	11.5	06.26	0.1067	15636	0.1067

^a Lattice parameters $a = 2.365$ nm, $b = 1.228$ nm, $c = 3.245$ nm.

^b According to the indexing scheme proposed by Yamamoto and Ishihara [18] with $a_d = 0.4507$ nm, and $c_d = 1.2283$ nm.

^c Weak intensities are not listed.

constants are half the size. The X-ray diffractogram is indexed using such a unit cell by referring to the correspondence between EDPs and X-ray diffraction diagram [19, 20]. The results are listed in Table I together with the indexation using d-phase notation for comparison. There are certain deviations of calculated lattice spacings (d values) from the experimental ones, and sometimes even much larger than the deviations calculated based on the d-phase model. Such an error may be in part introduced by lattice imperfections in the O-phase structure, as revealed most obviously by [0 1 0] EDP (a pattern in Fig. 7) which resembles the 10f pattern of the d-phase. The spots still tend to the positions of the d-phase, indicating that its structure is not far from that of the d-phase, in other words, the periodic ordering is not complete. Though resembling the d-phase, it is, however, truly a crystalline phase. Tilting around the 10f axis of the d-phase results in the successive appearances of P and D patterns at 18° intervals [21] while tilting around the [0 1 0] axis (a 2f axis) of O-phase results in different patterns ($e, f, g, h \dots$), although also at 18° intervals. Pattern f in Fig. 7 may be misleading because it is aperiodic in one 2f direction, rather like the pattern D of the d-phase. Fig. 8 presents the D pattern of d-phase to-

gether with a f pattern and a h pattern for the sake of comparison. It is easy to see that the aperiodic f pattern is different from pattern D in that it is not central symmetrical, which means that the diffraction spots do not lie exactly all on the same reciprocal plane. It is actually a reciprocal plane traversing a [0 1 0] axis and an irrational axis between [1 0 3] and [1 0 5] reciprocal directions as can be deduced from [0 1 0] EDP (a pattern in Fig. 7). This is made possible both by the huge size of the unit cell and by structural imperfections, the former making the reciprocal space very condensed and the latter making it distorted. Such a distortion is due to the existence of residues of its parent phase features in the O-phase structure, i.e. certain d-phase features are still retained, thus a schematic illustration is proposed as shown in Fig. 9 which takes the generation of the central column in f pattern as the projection of the nearby points lying roughly within the two dotted lines region on to an irrational axis between [1 0 3] and [1 0 5] reciprocal directions. Other aperiodic patterns like patterns g and i are due to the same cause.

The O-phase also has a stripy morphology similar to that of the d-phase. As shown in Fig. 10a, the grain size is usually up to several μm . Although single

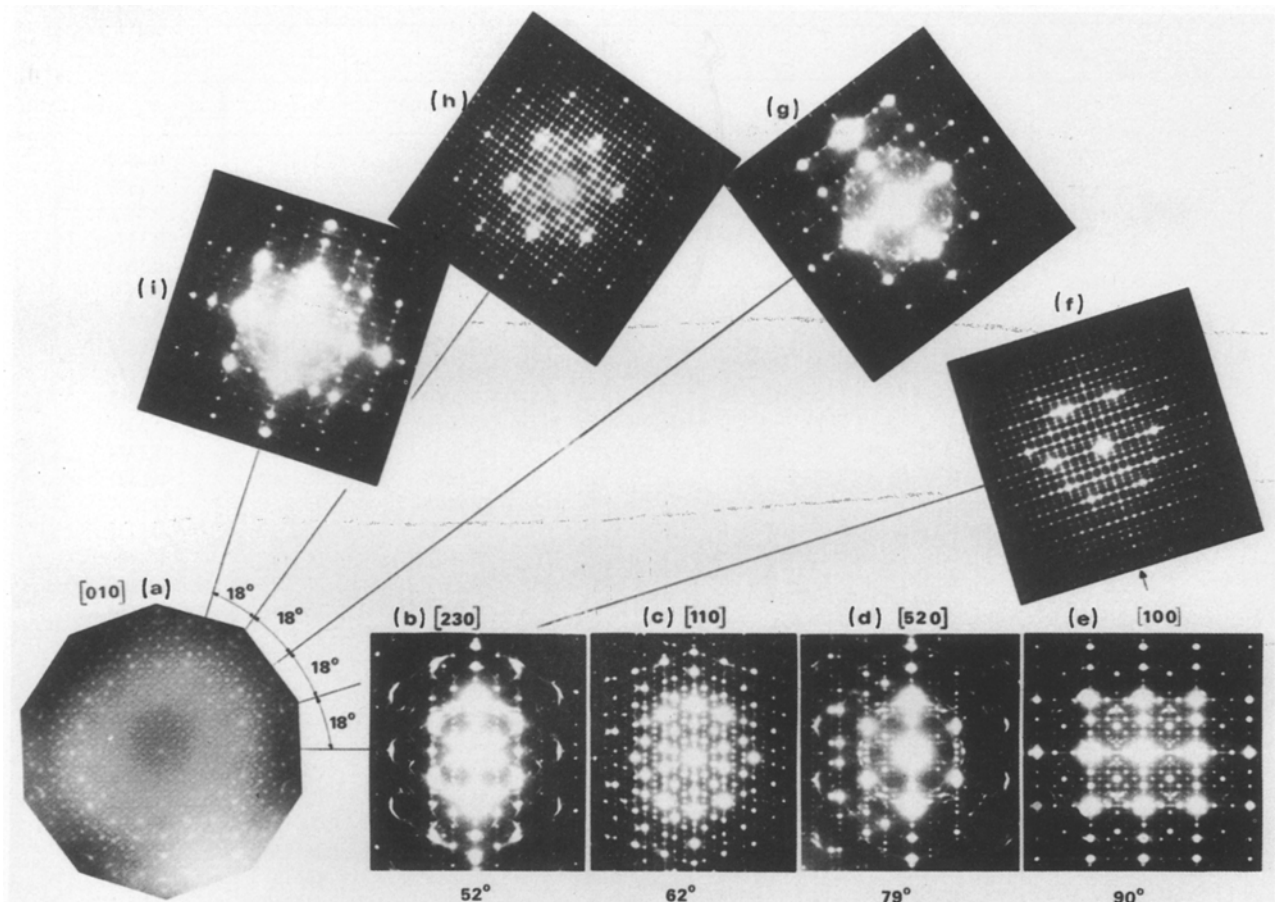


Figure 7 Stereo presentation of important diffraction patterns of O-phase obtained by double-tilting experiment. The spatial arrangement of these patterns is rather similar to that of decagonal phase.

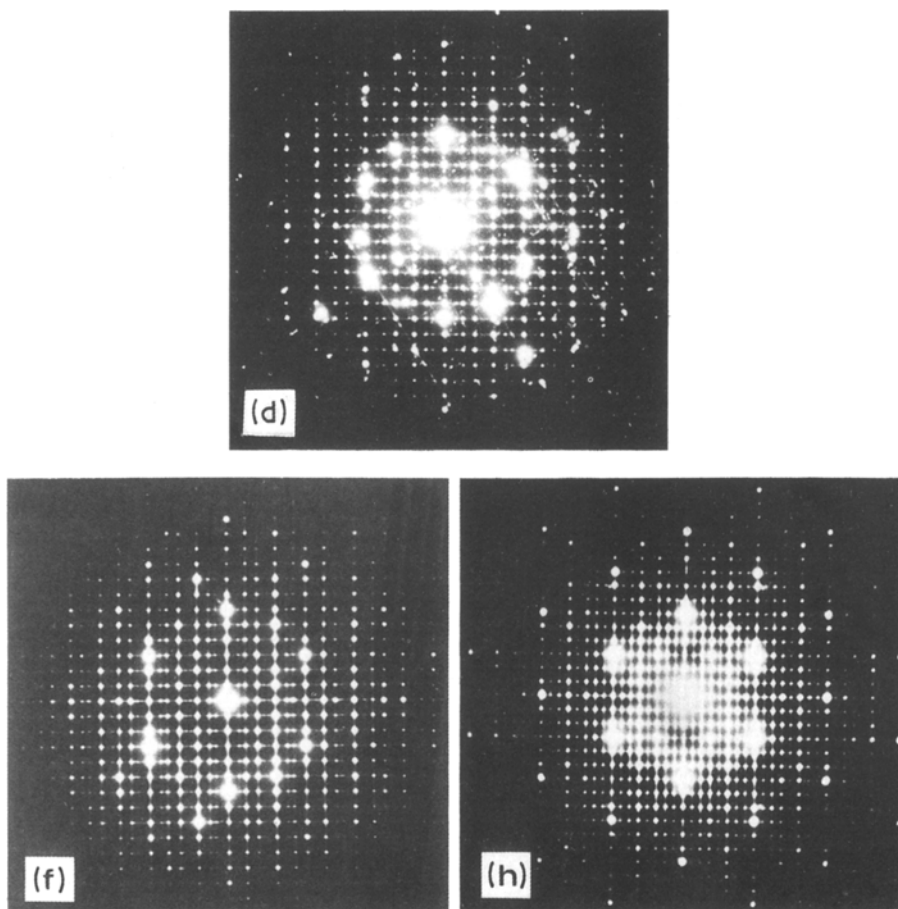


Figure 8 Comparison of D pattern of decagonal phase and with aperiodic *f* pattern and periodic *h* pattern of O-phase. It can be seen that *f* pattern is not central symmetrical. See text and Fig. 9 for explanation.

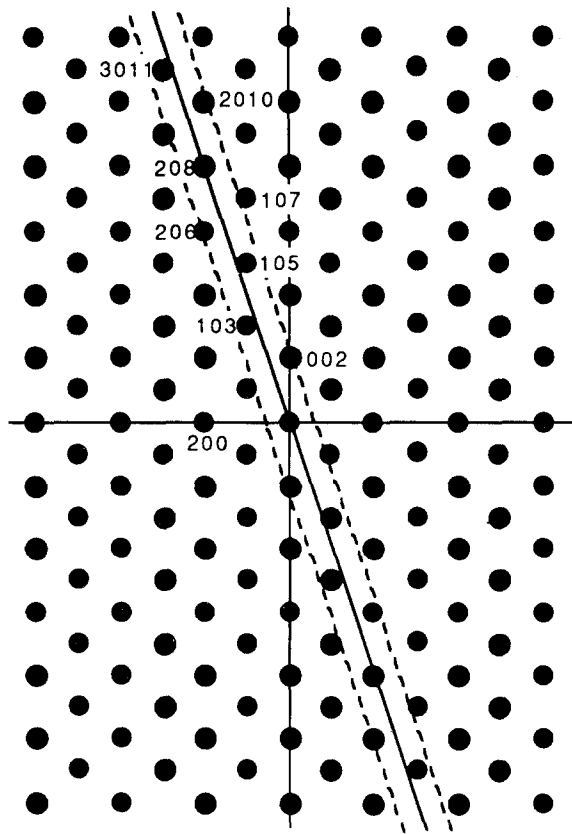


Figure 9 Geometrical illustration of the generation of the central column along a $2f$ axis indicated by an arrow in f pattern in Fig. 7. It is formed by projection of nearby spots on to an irrational axis between $[103]$ and $[105]$ reciprocal directions.

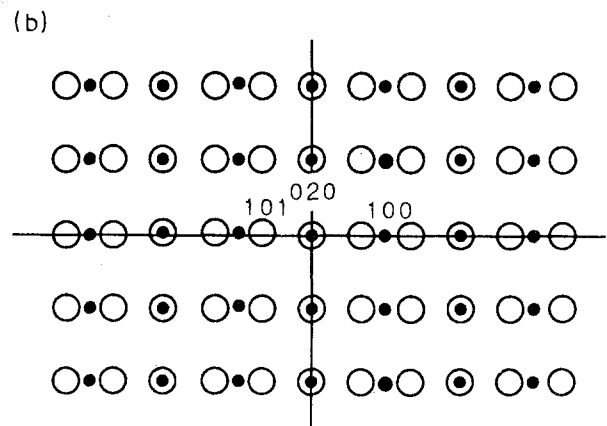
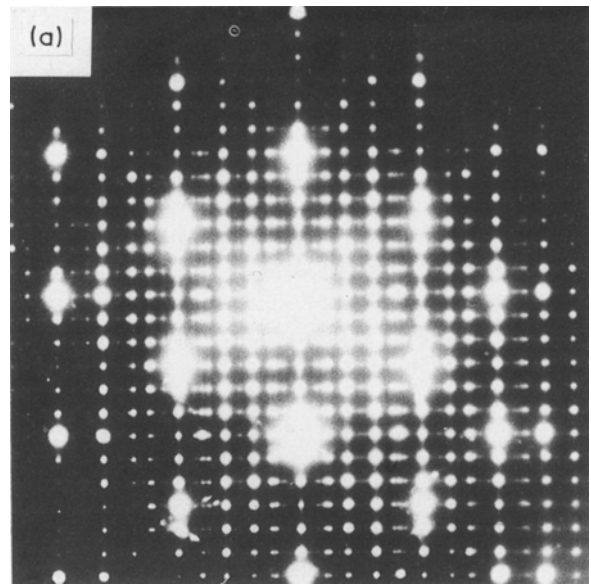


Figure 11 $[001]$ and $[10\bar{1}]$ Composite electron diffraction patterns of (a) O-phase and (b) their indexings.

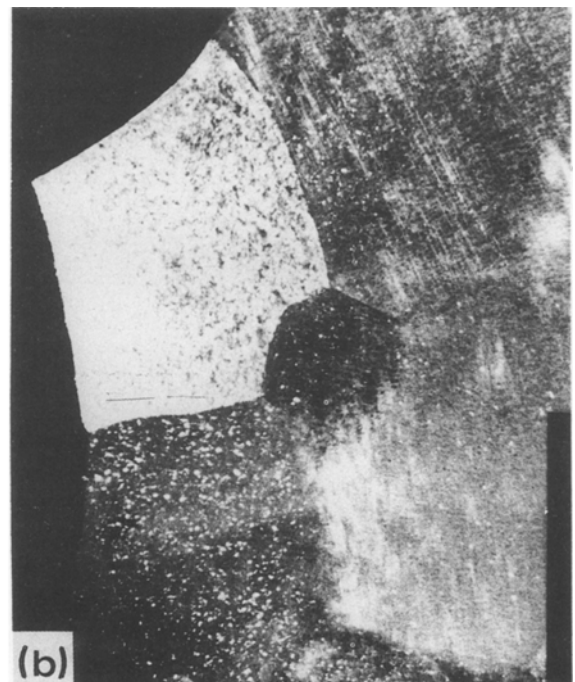
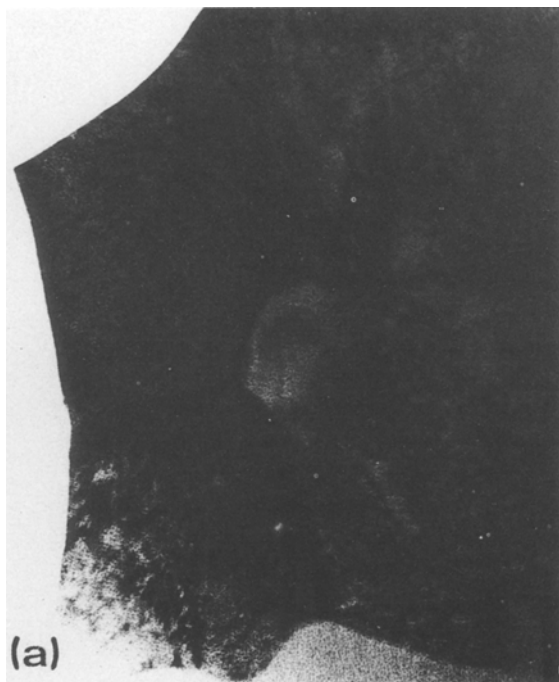


Figure 10 (a) Bright-field and (b) dark-field images taken from the sample after heat treatment. All are O-phase grains. The small particles are also O-phase, but with different orientations from the O-phase matrix.

crystal grains are not exceptional, small O-phase particles (tens of nanometres) on the O-phase matrix can often be seen as is clearly revealed by the dark-field image in Fig. 10b. There is a fixed relationship between the particles and the matrix. Fig. 11 is the composite EDP of $[10\bar{1}]$ and $[001]$ axes, the angle between them being 36° , therefore this relationship seems to suggest a 10f twinning with $[010]$, which corresponds to the 10f axis of the d-phase, as the twinning axis. This relation of the d-phase and 10f twin has been well established by Feng *et al.* [22] in Al-Fe spin-quenched sample where d-phase and 10f twins coexist.

4. Conclusions

The d-phase and i-phase are formed in the $\text{Al}_{65}\text{Cu}_{20}\text{Fe}_{10}\text{Cr}_5$ melt-spun ribbons, thus the structure of $\text{Al}_{65}\text{Cu}_{20}\text{Fe}_{15}$ alloy is sensitive to the additions of chromium which destabilize the i-phase and promote the formation of the d-phase. The equilibrium structure after sufficient heat treatment is a B centred orthorhombic phase, or O-phase as is named here, with lattice parameters $a = 2.365$ nm, $b = 1.228$ nm, $c = 3.250$ nm. O-phase is so closely related to the d-phase that normal X-ray measurement has failed to detect their difference. This point should be kept in mind when claiming the existence of quasicrystals only on the basis of X-ray diffraction measurements. It also demonstrates the ability of HREM to distinguish between microtwinning in crystals with large unit cells and truly aperiodic tiling in real quasicrystals.

Acknowledgements

One of us (C. D.) is indebted to the Institut Laue-Langevin (Grenoble) for financial support. The present work has benefited from the help of S. S. Kang and J. P. Houin. We are also grateful to C. Janot and M. de Boissieu for a long standing collaboration in the field of quasicrystals.

References

1. A. P. TSAI, A. INOUE and T. MASUMOTO, *Jpn J. Appl. Phys.* **26** (1987) L1505.
2. D. SHECHTMAN, I. BLECH, D. GRATIAS and J. W. CAHN, *Phys. Rev. Lett.* **53** (1984) 1951.
3. C. JANOT and J. M. DUBOIS, *J. Phys. F.* **18** (1988) 2303.
4. L. BENDERSKY, *Phys. Rev. Lett.* **55** (1985) 1461.
5. T. ISHMASA, H. V. NIESSEN and Y. FUKANO, *ibid.* **55** (1985) 511.
6. N. WANG, H. CHEN and K. H. KUO, *ibid.* **59** (1987) 1010.
7. D. SHECHTMAN, *Mater. Sci. Forum* **22-24** (1987) 1.
8. J. M. LANG, M. AUDIER, B. DUBOST and P. SAINFORT, *J. Crystallogr. Growth* **83** (1987) 456.
9. W. OHASHI and F. SPAEPEN, *Nature* **330** (1985) 555.
10. T. ISHMASA, Y. FUFANO and M. TSUCHIMORI, *Phil. Mag. Lett.* **583** (1988) 157.
11. Z. ZHANG and K. H. KUO, *J. Microsc.* (1987) **146** (1987) 313.
12. S. EBALARD and F. SPAEPEN, *J. Mater. Sci.* **24** (1989) 39.
13. R. J. SCHAEFER and L. BENDERSKY, *Scripta Metall.* **20** (1986) 745.
14. P. GUYOT and M. AUDIER, *J. Microsc. Spectrosc. Electron.* **10** (1985) 575.
15. N. THANGARAJ, G. N. SUBBOANNA, S. RANGA-NATHAN and K. CHATTOPADHYAY, *J. Microsc.* **146** (1987) 287.
16. J. REYES-GASGA and G. VAN TENDELOO, Proc. 3rd Workshop on Quasicrystals, Nancy, France, March 16-17, 1989 (unpublished).
17. K. YOSHIDA and A. TAKEKAWA, *Thin Solid Films* **48** (1978) 293.
18. A. YAMAMOTO and K. N. ISHIHARA, *Acta Crystallogr.* **A44** (1988) 707.
19. J. M. DUBOIS, C. JANOT, J. PANNETIER and A. PIANELLI, *Phys. Lett. A* **117** (1986) 42.
20. B. KOOPMANS, P. J. SCHURER and F. VAN DE WOUDE, *Phys. Rev. B* **35** (1987) 3005.
21. C. DONG, G. B. LI and K. H. KUO, *J. Phys. F.* **17** (1987) L189.
22. K. K. FENG, X. D. ZOU and C. Y. YANG, *Phil. Mag. Lett.* **55** (1987) 27.

Received 26 September 1989
and accepted 1 February 1990